

FAST RANDOMIZED ALGORITHMS FOR LOW-RANK MATRIX APPROXIMATIONS WITH APPLICATIONS IN GLOBAL COMPARATIVE ANALYSIS OF A CLASS OF DATA SETS *

WEIWEI XU [†], WEIJIE SHEN [‡], WEN LI [§], WEIGUO GAO [¶], AND YINGZHOU LI ^{||}

Abstract. Generalized singular values (GSVs) play an essential role in the comparative analysis. In the real world data for comparative analysis, both data matrices are usually numerically low-rank. This paper proposes a randomized algorithm to first approximately extract bases and then calculate GSVs efficiently. The accuracy of both basis extraction and comparative analysis quantities, angular distances, generalized fractions of the eigenexpression, and generalized normalized Shannon entropy, are rigorously analyzed. The proposed algorithm is applied to both synthetic data sets and the genome-scale expression data sets. Comparing to other GSVs algorithms, the proposed algorithm achieves the fastest runtime while preserving sufficient accuracy in comparative analysis.

Key words. Randomized algorithm, low-rank matrix approximations, comparative analysis, genome-scale expression data sets

AMS subject classifications. 68Q25, 68W20, 92B05

1. Introduction. The generalized singular value decomposition (GSVD) is a valuable and versatile mathematical tool in various scientific fields, including but not limited to, the general Gauss-Markov linear model, real-time signal processing, image processing. In the past decades, GSVD has played an essential role in the comparative analysis of genome-scale expression data, DNA-sequence, and mRNA-expression data [1, 2, 4, 5, 17]. Motivated by the comparative analysis, we propose a randomized method to accelerate the GSVD computation therein, which could be applied to other applications as well.

In the comparative analysis of expression data sets, we are given two expression data sets, G_1 and G_2 . The data sets G_1 and G_2 are of size m -genes \times n -arrays and p -genes \times n -arrays respectively. In order to distinguish the similarities and dissimilarities between two expression data sets, the GSVD is introduced as a mathematical tool. GSVD simultaneously transforms G_1 and G_2 to two reduced n -genelets \times n -arraylets spaces [1]. Then, various similarity measurements are adopted to compare the two data sets.

Throughout this paper, we adapt the following definitions of Grassman matrix pair (GMP) and GSVD [7, 14]. For $G_1 \in \mathbb{C}^{m \times n}$ and $G_2 \in \mathbb{C}^{p \times n}$, the matrix pair $\{G_1, G_2\}$ is an (m, p, n) *Grassman matrix pair* if $\text{rank}(G_1^H, G_2^H) = n$. Now we consider an (m, p, n) -GMP $\{G_1, G_2\}$. Its GSVD is defined as ¹,

$$G_1 = U \Sigma_{G_1} R, \quad G_2 = V \Sigma_{G_2} R, \quad (1.1)$$

where $U \in \mathbb{C}^{m \times n}$ and $V \in \mathbb{C}^{p \times n}$ are column orthogonal matrices, $R \in \mathbb{C}^{n \times n}$ is a nonsingular matrix, $\Sigma_{G_1} \in \mathbb{R}^{n \times n}$ and $\Sigma_{G_2} \in \mathbb{R}^{n \times n}$ are diagonal matrices with generalized singular values on their diagonals, i.e., $\Sigma_{G_1} = \text{diag } \alpha_1, \dots, \alpha_n$ and $\Sigma_{G_2} = \text{diag } \beta_1, \dots, \beta_n$ with

$$\begin{aligned} 1 = \alpha_1 = \dots = \alpha_r > \alpha_{r+1} \geq \dots \geq \alpha_{r+s} > \alpha_{r+s+1} = \dots = \alpha_n = 0, \\ 0 = \beta_1 = \dots = \beta_r < \beta_{r+1} \leq \dots \leq \beta_{r+s} < \beta_{r+s+1} = \dots = \beta_n = 1, \end{aligned} \quad (1.2)$$

and $\alpha_i^2 + \beta_i^2 = 1$ for $1 \leq i \leq n$. Here r and $n - r - s$ are numbers of zeros in $\{\beta_i\}$ and $\{\alpha_i\}$ respectively, and s counts the number that both α_i and β_i are not zeros. In the rest of the paper, we refer to s as the rank of the GSVD.

Once the GSVD of the expression data sets G_1 and G_2 is obtained, the matrix R defines the n -arraylets \times n -arrays basis transformation that is shared by both data sets. Matrices U and V define the m -genes \times n -genelets and p -genes \times n -genelets basis transformation for G_1 and G_2 respectively. With these basis transformations, the original comparison between G_1 and G_2 would be carried out by the comparison of $\{\alpha_i\}_{i=1}^n$ and $\{\beta_i\}_{i=1}^n$. The relative significance of the ℓ -th genelet, i.e., the significance of the ℓ -th genelet in G_1 compared to that in G_2 , is determined by the ratio of α_ℓ and β_ℓ . We denote the relative significance as

$$\rho_\ell = \frac{\alpha_\ell}{\beta_\ell}$$

*The research of this work was partially supported by the National Key R&D Program of China 2020YFA0711902, Natural Science Foundation of China under Grant No. 11971243, 12071159, 11690013, U1811464. This work was also supported in part by the major key project of Peng Cheng Laboratory under grant PCL2023AS1-2.

[†]School of Mathematics and Statistics, Nanjing University of Information Science and Technology, Nanjing 210044, China. The Peng Cheng Laboratory, Shenzhen 518055, China, and with the Pazhou Laboratory (Huangpu), Guangzhou 510555, China.

[‡]School of Mathematics and Statistics, Nanjing University of Information Science and Technology, Nanjing 210044, China.

[§]School of Mathematical Sciences, South China Normal University, Guangzhou 510631, China.

[¶]School of Mathematical Sciences and School of Data Science, Fudan University, Shanghai 200433, China.

^{||}School of Mathematical Sciences, Fudan University, Shanghai 200433, China.

¹This GSVD is actually reduced GSVD under the tall rectangular version, which is the one used in comparative analysis. Our proposed method is able to address non-reduced GSVD efficiently as well.

for $\ell = r + 1, \dots, n$, and $\rho_\ell = \infty$ for $\ell = 1, \dots, r$. Besides the relative significance, there are other measurements used in the comparative analysis: antisymmetric angular distance, generalized fractions of eigenexpression, and generalized normalized Shannon entropy.

The *antisymmetric angular distance* for the ℓ -th genelet between G_1 and G_2 is defined as,

$$\vartheta_\ell = \arctan\left(\frac{\alpha_\ell}{\beta_\ell}\right) - \frac{\pi}{4}. \quad (1.3)$$

An antisymmetric angular distance of $\vartheta_\ell = 0$ indicates that the ℓ -th genelet is of equal significance in both data sets. While, the distance $\vartheta_\ell = \pi/4$ indicates that the ℓ -th genelet in G_1 is significant relative to G_2 , whereas $\vartheta_\ell = -\pi/4$ indicates the other way around, i.e., the ℓ -th genelet in G_2 is significant relative to G_1 . The antisymmetric angular distances are ordered as $\pi/4 \geq \vartheta_1 \geq \dots \geq \vartheta_n \geq -\pi/4$.

The *generalized fractions of eigenexpression* of G_1 and G_2 are defined as,

$$P_{1,\ell} = \alpha_\ell^2 / \sum_{k=1}^n \alpha_k^2, \quad P_{2,\ell} = \beta_\ell^2 / \sum_{k=1}^n \beta_k^2, \quad (1.4)$$

respectively for $\ell = 1, \dots, n$. The generalized fractions of eigenexpression is not a relative distance between G_1 and G_2 . The fraction $P_{i,\ell}$ indicates the significance of the ℓ -th genelet in G_i for $i = 1, 2$. Note that the generalized fractions of eigenexpression $P_{1,\ell}$ and $P_{2,\ell}$ can be viewed as the probability that a genelet in G_1 and G_2 respectively.

The *generalized normalized Shannon entropy*,

$$D_i = \frac{-1}{\log n} \sum_{k=1}^n P_{i,k} \log P_{i,k}, \quad (1.5)$$

for $i = 1, 2$, defines an entropy measurement for the generalized fractions for G_1 and G_2 . By the property of entropy, we have $D_i \in [0, 1]$. The generalized normalized Shannon entropy measures the complexity of expression of genelets in the data set. If $D_i = 0$, then all expressions are captured by a single genelet in G_i . If $D_i = 1$, then expressions are in a disordered status, and all genelets in G_i are equally expressed.

Numerical methods of GSVD have been well developed. The GSVD of two real matrices was first proposed by Van Loan [10]. Paige and Saunders [14] used the CS decomposition of the unitary matrix to propose GSVD of matrix pair, which extended the real matrices in [10] to complex matrices. Bai and Demmel [3] described a variation of Paige's algorithm for computing the GSVD with an extra preprocessing step and a new algorithm in addressing 2×2 triangular GSVD. Stewart [15] and Van Loan [11] proposed two backward stable algorithms for computing the GSVD. Ewerbring and Luk [5] and Zha [17] extended GSVD for matrix triplets. Recently, Friedland [6] proposed a new GSVD algorithm, which suppresses the sensitivity to an error in the entries of the matrices. Xu et. al. [16] proposed the geometric inexact Newton method for generalized singular values of the Grassmann matrix pair. The GSVD of the matrix pair in MATLAB is calculated using the CS decomposition described in [7] and the built-in SVD and QR functions.

In this paper, we first propose a low-rank approximation algorithm based on random sampling technique with QR decomposition with pivoting. The randomized low-rank algorithm is then applied to approximately extract the column bases of G_1 and G_2 matrices. On top of the basis extraction, we propose algorithm 2 to obtain GSVs. The approximation accuracy of the basis extraction is analyzed in theorem 3.5 and the accuracy mainly depends on the decay property of the GSVs. Combined with the perturbation analysis of GSVs, we derive the accuracy analysis for quantities in comparative analysis. Finally, on both synthetic data sets and practical genome-scale expression data sets, the proposed algorithm shows advantages in runtime. And the accuracy is way beyond the desired ones in comparative analysis tasks.

The rest of the paper is organized as follows. In section 2, a randomized method is proposed to compute the GSVs of (m, p, n) -GMPs. Then, the generalized fractions of eigenexpression and generalized normalized Shannon entropy for comparative analysis of two data sets are calculated and analyzed in section 3. In section 4, numerical results for both synthetic data sets and practical yeast and human cell-cycle expression data sets are reported to demonstrate the efficiency of the proposed randomized method. Finally, section 5 concludes the paper with some discussions on future work.

2. Randomized algorithms for low-rank matrix approximations for GSVs. In this section, Gaussian random matrices are used to construct randomized algorithms with low-rank matrix approximations to remove the near-zero GSVs, either α or β , and reduce the overall computational cost. In the following, we first give a detailed description of our randomized algorithms for GSVs. Then, the computational cost comparison is discussed.

The randomized algorithm for GSVs is composed of two phases: 1) randomized algorithm for basis extraction; 2) calculating GSVs for compressed matrix pair.

The randomized algorithm for basis extraction aims to find an orthonormal basis sets for U and V in eq. (1.1) with non-zero GSVs α_i and β_j , respectively. Our randomized algorithm is essentially the same as the basis extraction algorithm in randomized SVD [12]. We need to apply the randomized algorithm to G_1 and G_2 , and obtain an approximated basis of U and V with non-zero GSVs. The difference mainly lies in the later analysis in section 3. Our goal of the randomized algorithm is approximating U and V whereas the original randomized SVD aims to approximate the left or right singular vectors of the matrix. Hence, as we will see later, the condition number of R would get into play in our approximation error analysis. In order to be self-contained, we will describe the randomized algorithm in extracting the basis.

Since the sizes of the approximated basis of U and V are unknown in a priori, we conduct an iterative scheme to obtain the basis batch by batch. We could also calculate the basis one by one, which is less efficient in modern computer architecture. Hence, we define a blocksize hyperparameter b controlling the batch size to benefit from the memory hierarchy efficiency. In many environments, picking b between 10 and 100 would be near optimal. [12] In our numerical experiments, we set b to be 100. For each iteration in the basis extraction, we apply the matrix to a Gaussian random matrix of size $m \times b$, followed by a projection matrix projecting out the bases from previous iterations. Then, we apply the reduced QR factorization to the matrix product result and obtain another batch of bases. We seek to build an orthonormal matrix Q such that

$$\|(I - QQ^H)G\|_F < \epsilon,$$

which is adopted as the stopping criterion. The square of the Frobinus norm of $G - QQ^HG$ could be calculated in a cumulated way efficiently. Hence, the dominant computational cost of the basis extraction algorithm lies in applying the matrix G to Gaussian random matrices. We summarize the basis extraction algorithm in algorithm 1.

Algorithm 1: Randomized algorithms for basis extraction

Input: Given an $m \times n$ matrix G , a tolerance ϵ and a blocksize integer number b .

Output: An approximated basis Q of U for $G = U\Sigma R$ as in eq. (1.1).

- 1: $Q = []$.
 - 2: **for** $i = 1$ to n/b **do**
 - 3: Let Ω_i be a Gaussian random matrix of size $n \times b$.
 - 4: Evaluate the projected matrix $Y_i = (I - QQ^H)(G\Omega_i)$.
 - 5: Compute the reduced QR decomposition $Y_i = P_i T_i$ for $P_i \in \mathbb{C}^{m \times b}$, $T_i \in \mathbb{C}^{b \times b}$.
 - 6: Append P_i to Q , i.e., $Q = [Q, P_i]$.
 - 7: **if** $\|(I - QQ^H)G\|_F < \epsilon$ **then**
 - 8: Return Q .
 - 9: **end if**
 - 10: **end for**
-

Then we aim to calculate GSVs for the compressed matrix pair and obtain the GSVD of the original matrix pair as in eq. (1.1). We now consider a scenario that generalized singular values are explicitly divided into three groups: exactly one, between one and zero, and exactly zero. Then the GSVD under the tall rectangular version admits,

$$G_1 = (U_1 \ U_2 \ U_3) \begin{pmatrix} I & & \\ & \tilde{\Sigma}_1 & \\ & & 0 \end{pmatrix} R, \quad G_2 = (V_1 \ V_2 \ V_3) \begin{pmatrix} 0 & & \\ & \tilde{\Sigma}_2 & \\ & & I \end{pmatrix} R. \quad (2.1)$$

The left bases of G_1, G_2 are Q_1, Q_2 . In the eq. (2.1), Q_1 is the basis of $(U_1 \ U_2)$ and orthogonal to U_3 , and Q_2 is the basis of $(V_2 \ V_3)$ and orthogonal to V_1 . Taking the projection of G_1 and G_2 on the basis of Q_1 and Q_2 respectively, we obtain,

$$\begin{pmatrix} G_1 \\ G_2 \end{pmatrix} = \begin{pmatrix} Q_1 Q_1^H G_1 \\ Q_2 Q_2^H G_2 \end{pmatrix} = \begin{pmatrix} Q_1 & \\ & Q_2 \end{pmatrix} \begin{pmatrix} Q_1^H G_1 \\ Q_2^H G_2 \end{pmatrix} = \begin{pmatrix} Q_1 & \\ & Q_2 \end{pmatrix} \begin{pmatrix} P_1 \begin{pmatrix} I & & 0 \\ & \tilde{\Sigma}_1 & 0 \end{pmatrix} R \\ P_2 \begin{pmatrix} 0 & & \\ & \tilde{\Sigma}_2 & \\ & & I \end{pmatrix} R \end{pmatrix}, \quad (2.2)$$

where $P_1 = Q_1^H (U_1 \ U_2)$ and $P_2 = Q_2^H (V_2 \ V_3)$ are square unitary matrices. The last equality in (2.2) obeys a general form of GSVD for $\begin{pmatrix} Q_1^H G_1 \\ Q_2^H G_2 \end{pmatrix}$. Hence the following phase calculates the GSVs for the compressed matrix pair $Q_1^H G_1$ and $Q_2^H G_2$. In the second algorithm, we apply reduced QR factorization to obtain the column basis of the matrix pair, and then calculate the GSVs from the basis directly. More precisely, let L_1 and L_2 be the top and bottom parts of the partial unitary matrix of the reduced QR factorization, i.e.,

$$\begin{pmatrix} Q_1^H G_1 \\ Q_2^H G_2 \end{pmatrix} = \begin{pmatrix} L_1 \\ L_2 \end{pmatrix} \tilde{R}.$$

where $L_1 \in \mathbb{C}^{l_1 \times n}$, $L_2 \in \mathbb{C}^{l_2 \times n}$ forms a partial unitary matrix, and $\tilde{R} \in \mathbb{C}^{n \times n}$ is an upper triangular matrix. The singular values of either L_1 or L_2 would reveal the GSVs of our original problem. Hence, we compute the singular values of the one of L_1 and L_2 with a smaller matrix size, and then calculate the GSV pairs. The overall algorithm is summarized in algorithm 2, where the basis extraction algorithm (algorithm 1) is denoted as ‘‘BasisExt’’, the tolerance and blocksize are passed to the function implicitly.

Algorithm 2: Randomized GSVs Algorithm

Input: Given matrix pair $G_1 \in \mathbb{C}^{m \times n}$, $G_2 \in \mathbb{C}^{p \times n}$.

Output: Generalized singular values $\{\alpha_i\}_{i=1}^n$, $\{\beta_i\}_{i=1}^n$.

1: $Q_1 = \text{BasisExt}(G_1)$.

2: $Q_2 = \text{BasisExt}(G_2)$.

3: Compute the reduced QR decomposition $\begin{pmatrix} Q_1^H G_1 \\ Q_2^H G_2 \end{pmatrix} = \begin{pmatrix} L_1 \\ L_2 \end{pmatrix} \tilde{R}$.

4: Denote numbers of rows of L_1 and L_2 as l_1 and l_2 respectively.

5: **if** $l_1 \leq l_2$ **then**

6: Compute the singular values L_1 , denoted as $\{\alpha_i\}_{i=1}^{l_1}$.

7: Append zeros $\alpha_i = 0$ for $i = l_1 + 1, \dots, n$.

8: Calculate $\beta_i = \sqrt{1 - \alpha_i^2}$ for $i = 1, \dots, n$.

9: **else**

10: Compute the singular values L_2 and sort them ascendingly, denoted as $\{\beta_i\}_{i=n-l_2+1}^n$.

11: Append zeros $\beta_i = 0$ for $i = 1, \dots, n - l_2$.

12: Calculate $\alpha_i = \sqrt{1 - \beta_i^2}$ for $i = 1, \dots, n$.

13: **end if**

If we want to recover the GSVD, we can do the following: Let the diagonal matrices composed of generalized singular values calculated by algorithm 2 be Σ_{G_1} and Σ_{G_2} . Let the singular value decomposition of L_1 and L_2 be $L_1 = U_1 \Sigma_{G_1} W_1$ and $L_2 = U_2 \Sigma_{G_2} W_2$ respectively. If $l_1 \leq l_2$, the matrices of GSVD of matrix pair $\{G_1, G_2\}$ are $U = Q_1 U_1$, $V = Q_2 L_2 W_1^{-1} \Sigma_{G_2}^{-1}$ and $R = W_1 \tilde{R}$ as in eq. (1.1). If $l_1 > l_2$, the matrices of GSVD of the matrix pair $\{G_1, G_2\}$ are $U = Q_1 L_1 W_2^{-1} \Sigma_{G_1}^{-1}$, $V = Q_2 W_2$ and $R = W_2 \tilde{R}$ as in eq. (1.1).

We now analyze the computational complexities of algorithm 1 and algorithm 2. In algorithm 1, the most expensive steps are the matrix-matrix multiplication (line 4). The computational cost could be estimated as

$$\sum_{i=1}^{l/b} O(mnb) = O(mnl),$$

where l is the number of columns in the output Q . The computational cost of algorithm 2 could be divided into three parts: basis extraction, reduced QR factorization, and SVD calculation. The basis extraction cost is the cost of algorithm 1 applying to G_1 and G_2 , and admits $O(mnl_1) + O(pl_2)$. The cost for SVD calculation is $O(n \min(l_1, l_2)^2)$. The cost for the reduced QR factorization step composed of two matrix-matrix multiplications and a QR factorization,

$$O(mnl_1) + O(pl_2) + O((l_1 + l_2)n^2),$$

which dominates the cost of the other two parts and is the overall cost for algorithm 2. In contrast, without basis compression, the cost of calculating the GSVs of the matrix pair G_1 and G_2 would be dominated by the QR factorization as that in algorithm 2, and admits,

$$O((m + p)n^2).$$

Consider a tall rectangular version of GSVD, the costs of GSVs calculations, with and without basis compression, differ by a ratio of $\max\{l_1, l_2\}/n$ in the complexity analysis. Further, the leading cost of algorithm 2 comes from the matrix-matrix multiplication, whereas that for GSVs without basis compression comes from the QR factorization. The extra prefactor difference between matrix-matrix multiplication and QR factorization is the extra saving for our proposed algorithm.

3. Comparative analysis of a class of genome-scale expression data sets. For a given matrix M , we write P_M for the unique orthogonal projector with $\text{range}(P_M) = \text{range}(M)$. When M has full column rank, we can express this projector explicitly

$$P_M = M(M^H M)^{-1} M^H.$$

In algorithm 1, for a matrix A , $A(:, i : j)$ denotes the submatrix from the i -th column to the j -th column in A , and $A(k, k)$ denotes the k -th diagonal element of A .

LEMMA 3.1. *Let Q_1 and ϵ be given by algorithm 1, then in step 7 there exist i such that $\|Q_1 Q_1^H G_1 - G_1\|_F < \epsilon$, and there exist j such that $\|Q_2 Q_2^H G_2 - G_2\|_F < \epsilon$.*

Proof. Here we only introduce the proof of G_1 in detail. Assume that $G_1 \Omega$ has the reduced QR decomposition

$$G_1 \Omega = G_1(\Omega_1, \dots, \Omega_{\frac{n}{b}}) = \tilde{Q} R = (\tilde{Q}_1, \dots, \tilde{Q}_{\frac{n}{b}}) R = (\tilde{Q}_1, \dots, \tilde{Q}_{\frac{n}{b}}) \begin{pmatrix} R_{11} & \cdots & R_{1, \frac{n}{b}} \\ & \ddots & \vdots \\ & & R_{\frac{n}{b}, \frac{n}{b}} \end{pmatrix},$$

where Ω_i is the $n \times b$ submatrix of Ω . When $i = 1$, $Y_1 = G_1 \Omega_1$, Y_1 has the reduced QR decomposition $Y_1 = P_1 T_1$. Due to Y_1 being a column full rank matrix, the QR decomposition of Y_1 is unique. Observe that $P_1 = \tilde{Q}_1$, $T_1 = R_{11}$. When $i = 2$, $Y_2 = G_1 \Omega_2 - \tilde{Q}_1 \tilde{Q}_1^H G_1 \Omega_2$ has the reduced QR decomposition $Y_2 = P_2 T_2$. For $G_1(\Omega_1, \Omega_2) = (\tilde{Q}_1, \tilde{Q}_2) \begin{pmatrix} R_{11} & R_{12} \\ 0 & R_{22} \end{pmatrix}$. It follows that

$$G_1 \Omega_1 = \tilde{Q}_1 R_{11}, G_1 \Omega_2 = \tilde{Q}_1 R_{12} + \tilde{Q}_2 R_{22}$$

and

$$\begin{aligned} \begin{pmatrix} R_{11} & R_{12} \\ 0 & R_{22} \end{pmatrix} &= \begin{pmatrix} \tilde{Q}_1^H \\ \tilde{Q}_2^H \end{pmatrix} \begin{pmatrix} \tilde{Q}_1 & \tilde{Q}_2 \end{pmatrix} \begin{pmatrix} R_{11} & R_{12} \\ 0 & R_{22} \end{pmatrix} = \begin{pmatrix} \tilde{Q}_1^H \\ \tilde{Q}_2^H \end{pmatrix} (G_1 \Omega_1 \quad G_1 \Omega_2) \\ &= \begin{pmatrix} \tilde{Q}_1^H G_1 \Omega_1 & \tilde{Q}_1^H G_1 \Omega_2 \\ \tilde{Q}_2^H G_1 \Omega_1 & \tilde{Q}_2^H G_1 \Omega_2 \end{pmatrix}. \end{aligned}$$

Observe that $\tilde{Q}_2 R_{22} = G_1 \Omega_2 - \tilde{Q}_1 R_{12} = G_1 \Omega_2 - \tilde{Q}_1 \tilde{Q}_1^H G_1 \Omega_2$. Since Y_2 is a column full rank matrix, the QR decomposition of Y_2 is unique. So $P_2 = \tilde{Q}_2$, $T_2 = R_{22}$. The same is true when $i > 2$. Therefore, $P_i = \tilde{Q}_i$, $1 \leq i \leq \frac{n}{b}$.

By algorithm 1 if $i = \frac{n}{b}$, then $Q_1 = [P_1, \dots, P_{\frac{n}{b}}] = [\tilde{Q}_1, \dots, \tilde{Q}_{\frac{n}{b}}]$. Since Ω is an $n \times n$ standard Gaussian matrix with $\text{rank} \Omega = n$, then by $G_1 \Omega = (\tilde{Q}_1, \dots, \tilde{Q}_{\frac{n}{b}}) R = Q_1 R$ we have $G_1 = Q_1 R \Omega^{-1}$. Hence, $Q_1 Q_1^H G_1 = Q_1 Q_1^H Q_1 R \Omega^{-1} = Q_1 R \Omega^{-1} = G_1$. Then there exist Q_1 such that for precision ϵ we have $\|Q_1 Q_1^H G_1 - G_1\|_F < \epsilon$. \square

Next, we will analyze the accuracy of the basis extraction.

PROPOSITION 3.2 (Proposition 10.1 [8]). *Fix matrices S, T , and draw a standard Gaussian matrix G . Then*

$$\mathbb{E} \|SGT\|_F^2 = \|S\|_F \|T\|_F.$$

PROPOSITION 3.3 (Proposition 10.2 [8]). *Draw a $k \times (k + p)$ standard Gaussian matrix G with $k \geq 2$ and $p \geq 2$. Then*

$$\mathbb{E} \|G^\dagger\|_F^2 = \frac{k}{p-1}.$$

THEOREM 3.4 (Theorem 3.3.16 [9]). *Let $A, B \in \mathbb{C}^{m \times n}$ be given. The following inequalities hold for the decreasingly ordered singular values of A, B and AB^H .*

$$\sigma_i(AB^H) \leq \sigma_i(A) \sigma_1(B), \quad i = 1, 2, \dots, \min\{m, n\}.$$

THEOREM 3.5. *Let $G_1 \in \mathbb{C}^{m \times n}$ and $G_2 \in \mathbb{C}^{p \times n}$ satisfy eq. (1.1), the target ranks $k_1, k_2 \geq 2$ and the oversampling parameters $p_1, p_2 \geq 2$ obey $k_1 + p_1 \leq \min\{m, n\}$, $k_2 + p_2 \leq \min\{p, n\}$, and $\Omega_1 \in \mathbb{C}^{n \times (k_1 + p_1)}$ and $\Omega_2 \in \mathbb{C}^{n \times (k_2 + p_2)}$ be standard Gaussian matrices. Denote φ_i and χ_i as GSVs of $\{G_1, G_2\}$. For $Q_1 \in \mathbb{C}^{m \times (k_1 + p_1)}$ and $Q_2 \in \mathbb{C}^{p \times (k_2 + p_2)}$ calculated by algorithm 1, we have*

$$\mathbb{E} \|(I_m - Q_1 Q_1^H) G_1\|_F^2 \leq \eta \left(\frac{k_1}{p_1 - 1} + 1 \right) \sum_{j > k_1}^n \varphi_j^2, \quad \text{and}$$

$$\mathbb{E} \|(I_p - Q_2 Q_2^H) G_2\|_F^2 \leq \eta \left(\frac{k_2}{p_2 - 1} + 1 \right) \sum_{j > k_2}^n \chi_{n-j+1}^2,$$

where $\eta = \sigma_{\max}(G_1^H G_1 + G_2^H G_2)$.

Proof. Throughout this proof, we focus on the analysis of G_1 and Q_1 and omit the subscript for simplicity. We inherit the GSVD of $\{G_1, G_2\}$ as in eq. (1.1). Let the SVD of G be $G = \hat{U} \hat{\Sigma} \hat{V}^H$. Then, we have,

$$G(G_1^H G_1 + G_2^H G_2)^{-\frac{1}{2}} = \hat{U} \hat{\Sigma} \hat{V}^H (G_1^H G_1 + G_2^H G_2)^{-\frac{1}{2}} = U \Sigma_G W,$$

where $W = R(R^H R)^{-\frac{1}{2}}$ is a unitary matrix. Rewriting $\hat{\Sigma}$ in terms of Σ_G , we obtain,

$$\hat{\Sigma} = \hat{U}^H U \Sigma_G W (G_1^H G_1 + G_2^H G_2)^{\frac{1}{2}} \hat{V}.$$

The SVD of G could be rewritten as top and bottom parts,

$$G = \hat{U} \hat{\Sigma} \hat{V}^H = \hat{U} \begin{pmatrix} \hat{\Sigma}_t & \\ & \hat{\Sigma}_b \end{pmatrix} \begin{pmatrix} \hat{V}_t^H \\ \hat{V}_b^H \end{pmatrix}, \quad (3.1)$$

where $\hat{\Sigma}_t \in \mathbb{R}^{k \times k}$ is a diagonal matrix with the largest k GSVs of G on the diagonal, $\hat{\Sigma}_b \in \mathbb{R}^{(m-k) \times (n-k)}$ is a diagonal matrix with the rest GSVs on the diagonal, $\hat{V}_t \in \mathbb{C}^{n \times k}$ and $\hat{V}_b \in \mathbb{C}^{n \times (n-k)}$ form a compatible top-bottom partition of \hat{V} .

By the unitary invariant property of the Frobinius norm, we have,

$$\begin{aligned} \|(I - Q Q^H) G\|_F &= \left\| (I - \hat{U}^H P_Q \hat{U}) \hat{U}^H G \right\|_F \\ &= \left\| (I - \hat{U}^H P_{G\Omega} \hat{U}) \hat{U}^H G \right\|_F = \left\| (I - P_{\hat{U}^H G \Omega}) \hat{U}^H G \right\|_F, \end{aligned}$$

where $P_{\hat{U}^H G \Omega}$ denotes the projector formed by $\hat{U}^H G \Omega$. We further construct an approximated basis of $\hat{U}^H G \Omega$ as,

$$Z = \hat{U}^H G \Omega \Lambda^\dagger \hat{\Sigma}_t^{-1} = \begin{pmatrix} I \\ F \end{pmatrix},$$

where

$$\Lambda = \hat{V}_t^H \Omega, \quad F = \hat{\Sigma}_b \tilde{\Lambda} \Lambda^\dagger \hat{\Sigma}_t^{-1}, \quad \text{and } \tilde{\Lambda} = \hat{V}_b^H \Omega.$$

From the expression of Z , we have $\text{range}(Z) \subset \text{range}(\hat{U}^H G \Omega)$ and, hence, obtain

$$\|(I - Q Q^H) G\|_F = \left\| (I - P_{\hat{U}^H G \Omega}) \hat{U}^H G \right\|_F \leq \left\| (I - P_Z) \hat{U}^H G \right\|_F. \quad (3.2)$$

The projector $I - P_Z$ could be explicitly written in terms of F ,

$$I - P_Z = \begin{pmatrix} I - (I + F^H F)^{-1} & B \\ B^H & I - F(I + F^H F)^{-1} F^H \end{pmatrix},$$

where $B = -(I + F^H F)^{-1} F^H$. Since

$$I - (I + F^H F)^{-1} \preceq F^H F, \quad \text{and } I - F(I + F^H F)^{-1} F^H \preceq I,$$

we could give an upper bound for the projector $I - P_Z$,

$$I - P_Z \preceq \begin{pmatrix} F^H F & B \\ B^H & I \end{pmatrix}.$$

Then substituting the upper bound of $I - P_Z$ into eq. (3.2), we have

$$\begin{aligned} \|(I - QQ^H)G\|_F^2 &\leq \|(I - P_Z)\hat{\Sigma}\hat{V}^H\|_F^2 = \|(I - P_Z)\hat{\Sigma}\|_F^2 \\ &\leq \text{tr} \left(\begin{pmatrix} \hat{\Sigma}_t & \\ & \hat{\Sigma}_b \end{pmatrix} \begin{pmatrix} F^H F & B \\ B^H & I \end{pmatrix} \begin{pmatrix} \hat{\Sigma}_t & \\ & \hat{\Sigma}_b \end{pmatrix} \right) = \|F\hat{\Sigma}_t\|_F^2 + \|\hat{\Sigma}_b\|_F^2. \end{aligned}$$

Taking the expectation with respect to the randomness in Ω , we prove the inequality for $G = G_1$,

$$\mathbb{E} \|(I - QQ^H)G\|_F^2 \leq \mathbb{E} \|\hat{\Sigma}_b \tilde{\Lambda} \Lambda^\dagger\|_F^2 + \|\hat{\Sigma}_b\|_F^2,$$

where the definition of F is substituted. By the definition of Λ and $\tilde{\Lambda}$, they are the top and bottom parts of the unitary matrix \hat{V} applied to the standard Gaussian matrix Ω . Due to the property of the standard Gaussian matrix, we know that Λ and $\tilde{\Lambda}$ are independent. Hence, we compute this expectation by first conditioning on Λ and then computing the expectation with respect to Λ ,

$$\mathbb{E} \|\hat{\Sigma}_b \tilde{\Lambda} \Lambda^\dagger\|_F^2 = \mathbb{E} \left(\mathbb{E} \left[\|\hat{\Sigma}_b \tilde{\Lambda} \Lambda^\dagger\|_F^2 \middle| \Lambda \right] \right) = \mathbb{E} \left(\|\hat{\Sigma}_b\|_F^2 \|\Lambda^\dagger\|_F^2 \right) = \frac{k}{p-1} \cdot \|\hat{\Sigma}_b\|_F^2,$$

where the second equality is due to theorem 3.2 and the last equality is due to theorem 3.3.

Combined with singular value inequality theorem 3.4, we prove the first expectation inequality in the theorem,

$$\mathbb{E} \|(I - QQ^H)G\|_F^2 \leq \left(1 + \frac{k}{p-1}\right) \|\hat{\Sigma}_b\|_F^2 \leq \eta \left(1 + \frac{k}{p-1}\right) \sum_{j>k} \varphi_j^2,$$

where $\eta = \sigma_{\max}(R^H R) = \sigma_{\max}(G_1^H G_1 + G_2^H G_2)$. The second expectation inequality in the theorem could be proved similarly. \square

In the following, we estimate the numerical errors in comparative analysis quantities when the generalized singular values are perturbed. We stick to the following notations,

$$G = \begin{pmatrix} G_1 \\ G_2 \end{pmatrix}, \quad \tilde{G} = G + \Delta G = G + \begin{pmatrix} \Delta G_1 \\ \Delta G_2 \end{pmatrix} = \begin{pmatrix} \tilde{G}_1 \\ \tilde{G}_2 \end{pmatrix}.$$

The generalized singular value pairs (φ_i, χ_i) of $\{G_1, G_2\}$ and those $(\tilde{\varphi}_i, \tilde{\chi}_i)$ of $\{\tilde{G}_1, \tilde{G}_2\}$ be ordered as in eq. (1.2). The errors between φ_ν, χ_ν and $\tilde{\varphi}_\nu, \tilde{\chi}_\nu$ are denoted as $\Delta\varphi_\nu, \Delta\chi_\nu$ respectively.

From theorem 3.5, we know that the randomized GSVs algorithm could produce fairly accurate \tilde{G}_1 and \tilde{G}_2 for a small tolerance ϵ and relatively large k_1 and k_2 , hence, small ΔG . We introduce a new notation \mathcal{E} as,

$$\mathcal{E} = \sqrt{2} \|\Delta G\|_F \min \left\{ \|G^\dagger\|, \|\tilde{G}^\dagger\| \right\},$$

which will be used to bound the numerical errors for both GSVs and comparative analysis quantities.

LEMMA 3.6. [13] Assume $\text{rank } G = \text{rank } \tilde{G} = n$. Then

$$\sqrt{\sum_{i=1}^n [(\varphi_i - \tilde{\varphi}_i)^2 + (\chi_i - \tilde{\chi}_i)^2]} \leq \mathcal{E}.$$

Through a direct calculation, we could have the following error bounds based on theorem 3.6.

COROLLARY 3.7. Assume $\text{rank } G = \text{rank } \tilde{G} = n$. Then

$$|\Delta\varphi| \leq \mathcal{E} \quad \text{and} \quad |\Delta\chi| \leq \mathcal{E},$$

where $|\Delta\varphi| = \max_{1 \leq \nu \leq n} \{|\Delta\varphi_\nu|\}$ and $|\Delta\chi| = \max_{1 \leq \nu \leq n} \{|\Delta\chi_\nu|\}$.

THEOREM 3.8. Let $\vartheta_\nu, P_{1,\nu}, P_{2,\nu}, D_1$ and D_2 represent the exact values, and $\tilde{\vartheta}_\nu, \tilde{P}_{1,\nu}, \tilde{P}_{2,\nu}, \tilde{D}_1$ and \tilde{D}_2 represent the values calculated by algorithm 2, eq. (1.3), eq. (1.4) and eq. (1.5). Then for $\nu = 1, 2, \dots, n$,

$$\begin{aligned} (i) \quad & \left| \vartheta_\nu - \tilde{\vartheta}_\nu \right| \leq \arcsin(2\mathcal{E}), \\ (ii) \quad & \left| P_{1,\nu} - \tilde{P}_{1,\nu} \right| \leq \frac{2\varphi_\nu \mathcal{E}}{\sum_{k=1}^n \varphi_k^2} + o(\mathcal{E}) \quad \text{and} \quad \left| P_{2,\nu} - \tilde{P}_{2,\nu} \right| \leq \frac{2\chi_\nu \mathcal{E}}{\sum_{k=1}^n \chi_k^2} + o(\mathcal{E}), \\ (iii) \quad & \left| D_1 - \tilde{D}_1 \right| \leq 2\mathcal{E} \sum_{i=1}^n \left| \frac{\varphi_i}{\sum_{k=1}^n \varphi_k^2} \left(\log \frac{\varphi_i^2}{\sum_{k=1}^n \varphi_k^2} \frac{1}{\log n} + D_1 \right) \right| + o(\mathcal{E}) \quad \text{and} \\ & \left| D_2 - \tilde{D}_2 \right| \leq 2\mathcal{E} \sum_{i=1}^n \left| \frac{\chi_i}{\sum_{k=1}^n \chi_k^2} \left(\log \frac{\chi_i^2}{\sum_{k=1}^n \chi_k^2} \frac{1}{\log n} + D_2 \right) \right| + o(\mathcal{E}). \end{aligned}$$

Proof. Let $\varphi_\nu = \sin(\gamma_\nu)$, $\chi_\nu = \cos(\gamma_\nu)$, $\tilde{\varphi}_\nu = \varphi_\nu + \Delta\varphi_\nu = \sin(\gamma_\nu + \Delta\gamma_\nu)$ and $\tilde{\chi}_\nu = \chi_\nu + \Delta\chi_\nu = \cos(\gamma_\nu + \Delta\gamma_\nu)$, where $|\Delta\varphi_\nu| \leq 1$, $|\Delta\chi_\nu| \leq 1$, $\Delta\gamma_\nu$ is a perturbation. Without loss of generality, we denote $\Theta = \text{diag} \theta_1, \dots, \theta_n$ with $\theta_\nu = \varphi_\nu$ as the case for $l_1 \leq l_2$ in algorithm 2. Recall the expressions of $\vartheta_\nu, P_{i,\nu}$ and D_i in terms of θ_ν ,

$$\begin{aligned} \vartheta_\nu &= \arctan \left(\frac{\theta_\nu}{\sqrt{1 - \theta_\nu^2}} \right) - \frac{\pi}{4}, \quad P_{1,\nu} = \frac{\theta_\nu^2}{\text{tr}(\Theta^2)}, \quad P_{2,\nu} = \frac{1 - \theta_\nu^2}{n - \text{tr}(\Theta^2)}, \\ D_1 &= -\frac{1}{\log n} \left[\sum_{i=1}^n \frac{\theta_i^2}{\text{tr}(\Theta^2)} [2 \log \theta_i - \log(\text{tr}(\Theta^2))] \right], \\ D_2 &= -\frac{1}{\log n} \left[\sum_{i=1}^n \frac{1 - \theta_i^2}{n - \text{tr}(\Theta^2)} [\log(1 - \theta_i^2) - \log(n - \text{tr}(\Theta^2))] \right], \end{aligned}$$

for $\nu = 1, \dots, n$.

(i) By definitions of φ_ν, χ_ν and γ_ν , we obtain,

$$\begin{aligned} \gamma_\nu &= \arcsin(\varphi_\nu), \quad \gamma_\nu + \Delta\gamma_\nu = \arcsin(\varphi_\nu + \Delta\varphi_\nu) \quad \text{and} \\ \gamma_\nu &= \arccos(\chi_\nu), \quad \gamma_\nu + \Delta\gamma_\nu = \arccos(\chi_\nu + \Delta\chi_\nu). \end{aligned}$$

By trigonometric identities, the difference between the above equations admit,

$$\begin{aligned} \sin(\Delta\gamma_\nu) &= \sin(\arcsin(\varphi_\nu + \Delta\varphi_\nu) - \arcsin(\varphi_\nu)) \\ &= \sin \arcsin(\varphi_\nu + \Delta\varphi_\nu) \cos \arcsin(\varphi_\nu) - \cos \arcsin(\varphi_\nu + \Delta\varphi_\nu) \sin \arcsin(\varphi_\nu) \\ &= (\varphi_\nu + \Delta\varphi_\nu)\chi_\nu - (\chi_\nu + \Delta\chi_\nu)\varphi_\nu \\ &= \Delta\varphi_\nu\chi_\nu - \Delta\chi_\nu\varphi_\nu. \end{aligned}$$

Adopting the inequalities in theorem 3.7 and the equality recursively, we obtain

$$\sin \left| \vartheta_\nu - \tilde{\vartheta}_\nu \right| = |\sin(\Delta\gamma_\nu)| \leq |\Delta\varphi_\nu| + |\Delta\chi_\nu| \leq 2\mathcal{E},$$

and, hence,

$$\left| \vartheta_\nu - \tilde{\vartheta}_\nu \right| \leq \arcsin(2\mathcal{E}).$$

(ii) By the Taylor expansion of $P_{1,\nu}$ at $(\varphi_1, \varphi_2, \dots, \varphi_n)$, we obtain

$$\left| \tilde{P}_{1,\nu} - P_{1,\nu} \right| = \left| \sum_{\nu=1}^n \Delta\varphi_\nu \frac{\partial P_{1,\nu}}{\partial \varphi_\nu} + o(\Delta\varphi_\nu) \right| \leq |\Delta\varphi| \frac{2\varphi_\nu \sum_{k \neq \nu} \varphi_k^2}{(\sum_{k=1}^n \varphi_k^2)^2} + o(\Delta\varphi) \leq \frac{2\mathcal{E}\varphi_\nu}{\sum_{k=1}^n \varphi_k^2} + o(\mathcal{E}),$$

where the second inequality adopts theorem 3.7. The bound for $\left| \tilde{P}_{2,\nu} - P_{2,\nu} \right|$ could be derived similarly.

(iii) By the Taylor expansion of D_1 at $(\varphi_1, \varphi_2, \dots, \varphi_n)$,

$$\tilde{D}_1 = D_1 + \sum_{i=1}^n \Delta\varphi_i \frac{\partial D_1}{\partial \varphi_i} + o(\Delta\varphi_i),$$

where

$$\begin{aligned}
\frac{\partial D_1}{\partial \varphi_i} &= -\frac{1}{\log n} \left[\frac{2\varphi_i}{\sum_{k=1}^n \varphi_k^2} \left(\log \frac{\varphi_i^2}{\sum_{k=1}^n \varphi_k^2} + 1 \right) - \sum_{j=1}^n \frac{2\varphi_i \varphi_j^2}{(\sum_{k=1}^n \varphi_k^2)^2} \left(\log \frac{\varphi_j^2}{\sum_{k=1}^n \varphi_k^2} + 1 \right) \right] \\
&= -\frac{1}{\log n} \left[\frac{2\varphi_i}{\sum_{k=1}^n \varphi_k^2} \left(\log \frac{\varphi_i^2}{\sum_{k=1}^n \varphi_k^2} + 1 \right) - \frac{2\varphi_i}{\sum_{k=1}^n \varphi_k^2} (D_1 \log n + 1) \right] \\
&= -\frac{1}{\log n} \left[\frac{2\varphi_i}{\sum_{k=1}^n \varphi_k^2} \left(\log \frac{\varphi_i^2}{\sum_{k=1}^n \varphi_k^2} + D_1 \log n \right) \right].
\end{aligned}$$

We obtain

$$\begin{aligned}
|D_1 - \tilde{D}_1| &= \left| \sum_{i=1}^n \Delta \varphi_i \frac{\partial D_1}{\partial \varphi_i} + o(\Delta \varphi_i) \right| \leq |\Delta \varphi| \left| \sum_{i=1}^n \frac{\partial D_1}{\partial \varphi_i} \right| + o(\Delta \varphi) \\
&\leq 2\mathcal{E} \sum_{i=1}^n \left| \frac{\varphi_i}{\sum_{k=1}^n \varphi_k^2} \left(\log \frac{\varphi_i^2}{\sum_{k=1}^n \varphi_k^2} \frac{1}{\log n} + D_1 \right) \right| + o(\mathcal{E}),
\end{aligned}$$

where second inequality adopts theorem 3.7.

The bound for $|\tilde{D}_2 - D_2|$ could be derived similarly. \square

4. Numerical experiments. We apply algorithm 2 in comparative analysis of both synthetic data sets and genome-scale expression data sets from practice. Comparative analysis quantities, $\vartheta_\nu, P_{i,\nu}, D_i$ for $i = 1, 2$ and $1 \leq \nu \leq n$, are evaluated following a GSV calculation. All numerical experiments are carried out on MATLAB R2021b with machine epsilon being around 2.2204×10^{-16} . By default, we adopt MATLAB `gsvd` results as refernces. The source code of our method is released at <https://github.com/shenwj87/RGSVsA.git>.

4.1. Synthetic data sets. Synthetic data sets are adopted to demonstrate the efficiency of algorithm 2. We compare algorithm 2 with the algorithm in [6], Riemann Newton (RN) method [16], the MATLAB built-in functions `gsvd` and `economy-sized gsvd`.

The synthetic data sets are generated as follows. Here we give the rank of G_1 and the rank of G_2 both being 60% of $\min\{m, p, n\}$. The generalized singular values that are neither one nor zero among $\alpha_1^*, \dots, \alpha_n^*$ are sampled from a random uniform distribution after sorting. Then β_i^* is calculated such that $(\alpha_i^*)^2 + (\beta_i^*)^2 = 1$ for $1 \leq i \leq n$. The nonsingular matrix $R_\star \in \mathbb{C}^{n \times n}$ is an n -by- n matrix of normally distributed random complex numbers. The unitary matrices $U_\star \in \mathbb{C}^{m \times n}$, $V_\star \in \mathbb{C}^{p \times n}$ are orthonormalized Gaussian random complex matrices. The data set $\{G_1, G_2\}$ is then $G_1 = U_\star \Sigma_1^* R_\star$ and $G_2 = V_\star \Sigma_2^* R_\star$, where $\Sigma_1^* = \text{diag } \alpha_1^*, \dots, \alpha_n^*$ and $\Sigma_2^* = \text{diag } \beta_1^*, \dots, \beta_n^*$. Various (m, p, n) choices are explored. Absolute errors of GSVs are used to compare the accuracy of GSV algorithms. Numerical results are reported in fig. 1, table 1, and fig. 2.

In table 1, we could observe the advantage of algorithm 2 both in runtime and accuracy. The runtimes of algorithm 2 are the shortest in all cases we have tested. In some cases, it is 10x to 20x faster than the second-fastest algorithm. In the least case, algorithm 2 saves about 20% runtime. Regarding accuracy, algorithm 2 achieves the best accuracy in most of the cases. In the worst case, algorithm 2 achieves 10^{-10} absolute accuracy comparing to 10^{-12} of the best. Such an accuracy is sufficient in almost all applications.

In fig. 1, we explore the performance of various GSV algorithms on matrices with increasing n . According to three figures in the right column of fig. 1, algorithm 2 achieves sufficiently high accuracy for comparative analysis problems. Algorithm 2, as in the left column of fig. 1, is the fastest among five algorithms. As the matrix size increases, the runtime gap between algorithm 2 and other algorithms further enlarges.

As shown in fig. 2, when the basis approximation error $\|G_i - Q_i Q_i^H G_i\|_F$ decreases, the absolute errors of GSVs $\|\Sigma_i^* - \Sigma_i\|_F$ decrease for $i = 1, 2$. If only a few digits of accuracy is needed for GSVs, which is the usual case in practice, we could adopt a small number of bases in the approximation, i.e., Q_i with a small number of columns. The computational cost could then be further reduced.

4.2. Genome-scale expression data sets. Algorithm 2 is applied to two practical genome-scale expression data sets in this section: yeast and human cell-cycle expression data set and mice macrophage gene expression data set.

TABLE 1
Runtime (second) and absolute errors for synthetic data sets. The shortest runtimes are bolded.

(m, p, n)	Algorithm	Runtime	$\ \Sigma_1^* - \Sigma_1\ _F$	$\ \Sigma_2^* - \Sigma_2\ _F$
(10000,10000,10000)	algorithm 2	105.48	4.45E-12	3.10E-11
	economy-sized gsvd	377.82	3.88E-12	3.13E-12
	gsvd	365.21	3.88E-12	3.13E-13
	Algorithm in [6]	1220.28	1.36E-09	4.12E-09
	RN method [16]	375.81	1.02E-12	2.35E-12
(8010,4005,4000)	algorithm 2	16.06	4.45E-14	1.27E-12
	economy-sized gsvd	22.83	9.19E-12	7.82E-12
	gsvd	49.50	9.51E-12	6.44E-12
	Algorithm in [6]	63.82	6.84E-09	5.66E-09
	RN method [16]	36.27	1.59E-12	1.00E-12
(9010,9005,5000)	algorithm 2	36.90	6.82E-14	7.20E-14
	economy-sized gsvd	44.97	8.22E-12	7.93E-12
	gsvd	61.42	8.50E-12	7.25E-12
	Algorithm in [6]	158.44	7.19E-09	3.62E-09
	RN method [16]	57.71	1.60E-12	1.36E-12
(8000,8010,8005)	algorithm 2	74.29	3.65E-10	6.36E-10
	economy-sized gsvd	150.78	5.06E-12	4.65E-12
	gsvd	189.10	4.79E-12	3.92E-12
	Algorithm in [6]	647.37	1.08E-05	1.04E-05
	RN method [16]	165.87	1.46E-12	1.72E-12
(10000,5010,5000)	algorithm 2	6.45	1.78E-15	1.65E-15
	economy-sized gsvd	41.21	2.69E-12	2.21E-12
	gsvd	48.93	2.84E-12	1.78E-12
	Algorithm in [6]	175.65	8.76E-06	1.82E-05
	RN method [16]	44.79	2.72E-12	2.46E-12
(10010,5000,10000)	algorithm 2	8.87	2.20E-15	2.04E-15
	economy-sized gsvd	197.49	2.36E-12	2.90E-12
	gsvd	175.78	2.89E-12	2.44E-12
	Algorithm in [6]	298.85	5.20E-08	4.28E-08
	RN method [16]	182.62	2.67E-12	2.85E-12
(7000,7010,10000)	algorithm 2	56.21	3.39E-14	3.77E-14
	economy-sized gsvd	117.85	2.78E-12	1.51E-12
	gsvd	118.75	2.80E-12	2.57E-12
	Algorithm in [6]	429.30	3.76E-07	3.71E-07
	RN method [16]	118.06	2.93E-12	2.86E-12
(5000,10000,11000)	algorithm 2	133.75	1.39E-14	1.46E-15
	economy-sized gsvd	195.23	1.17E-12	2.40E-12
	gsvd	192.18	1.09E-12	3.72E-12
	Algorithm in [6]	1110.65	4.40E-07	4.31E-07
	RN method [16]	194.31	6.11E-12	8.14E-12

4.2.1. Yeast and human cell-cycle expression data set. A yeast and human cell-cycle expression data set is adopted, which is available at <http://genome-www.stanford.edu/GSVD/>. In this data set, 4523-genes \times 18-arrays are analyzed for yeast and 12056-genes \times 18-arrays are analyzed for human. Hence, the matrix G_1 and G_2 are of size 4523 \times 18 and 12056 \times 18, respectively. Numerically, we validate that matrix G_1 , G_2 , and $\begin{pmatrix} G_1 \\ G_2 \end{pmatrix}$ are of full column rank. Notice that some data in the data set are missing. We adopt two methods [2], the SVD interpolation and spline, to recover these data. The runtimes of various algorithms are reported in table 2 and the accuracies of algorithm 2 for various comparative analysis quantities are given in table 3. Figure 3 and fig. 4

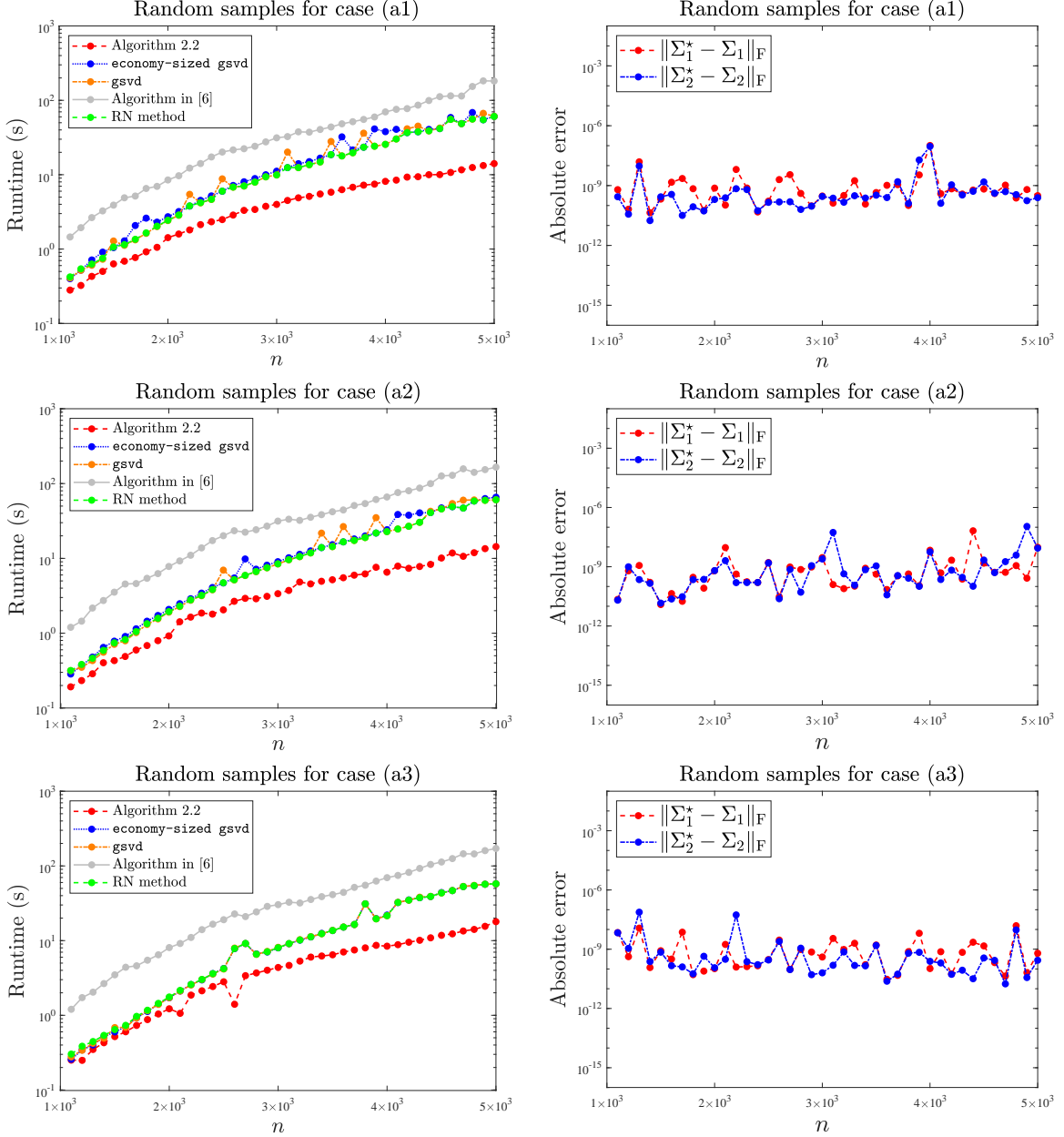


FIG. 1. Runtime (second) and absolute errors for cases of (m, p, n) . (a1) with $m = n + 100$ and $p = n + 5$; (a2) with $m = n + 100$ and $p = n - 5$; (a3) with $m = n - 100$ and $p = n - 5$.

illustrate the comparative analysis quantities of the SVD interpolation and spline methods, respectively.

Table 2 shows that the proposed algorithm algorithm 2 is about five times faster than the second fastest algorithms. The absolute accuracies obtained by algorithm 2, as shown in table 3, are all around machine epsilon, which is accurate enough in practical comparative analysis. In this data set, the number of columns, i.e., n , is much smaller than m and p . Hence, both G_1 and G_2 matrices are tall-and-skinny. All explored algorithms except `gsvd` benefit from the tall-and-skinny property in the data set and their runtimes are significantly smaller than that of `gsvd`.

According to fig. 3 and fig. 4, yeast generalized fractions of eigenexpression shows that the first two arrays capture more than 12% of the overall yeast expression and human generalized fractions of eigenexpression shows that the last array captures about 9%. When different missing data recovery methods are adopted, the comparative analysis results differ slightly. When the SVD interpolation is adopted, the sixth array is equally significant in both data sets with $\vartheta_6 \approx 0$. When the spline is adopted, the ϑ of the fifth array is the most close to zero.

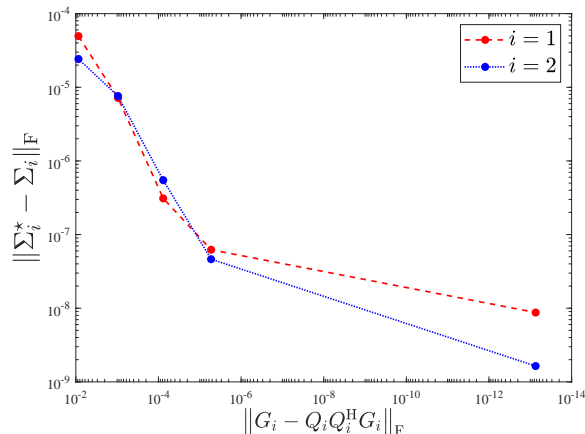


FIG. 2. Relation between $\|G_i - Q_i Q_i^H G_i\|_F$ and $\|\Sigma_i^* - \Sigma_i\|_F$, for $i = 1, 2$.

TABLE 2

Runtime (second) of algorithms on the yeast and human cell-cycle expression data set with SVD interpolation and spline.

Algorithm	SVD interpolation	Spline
algorithm 2	0.000481	0.000470
economy-sized gsvd	0.003390	0.003914
gsvd	3.808657	3.607354
Algorithm in [6]	0.002306	0.002280
RN method [16]	0.003321	0.003868

4.2.2. Mice macrophage gene expression data set. After the mice macrophage with Polyamide (PA) and RPMI1640 medium (containing phenol red) experiment, we can obtain data sets of the gene mRNA expression level. This data set for mice macrophage with Polyamide (PA) stimulation tabulates the matrix of size 22580-genes \times 9000-arrays and with RPMI1640 medium tabulates the matrix of size 22580-genes \times 9000-arrays. Compared to the data set in section 4.2.1, the data set in this section has much comparable m , p , and n . data. The runtimes of various algorithms are reported in table 4 and the accuracies of algorithm 2 for various comparative analysis quantities are given in table 5. Figure 5 illustrates the histogram of comparative analysis quantities.

Table 4 shows that the proposed algorithm algorithm 2 is at least one hundred times faster than all other algorithms. The runtimes of other algorithms in this data set are beyond 10 hours. While algorithm 2 could obtain desired results in less than 10 mins. The absolute accuracies obtained by algorithm 2, as shown in table 5, are all around 10^{-12} .

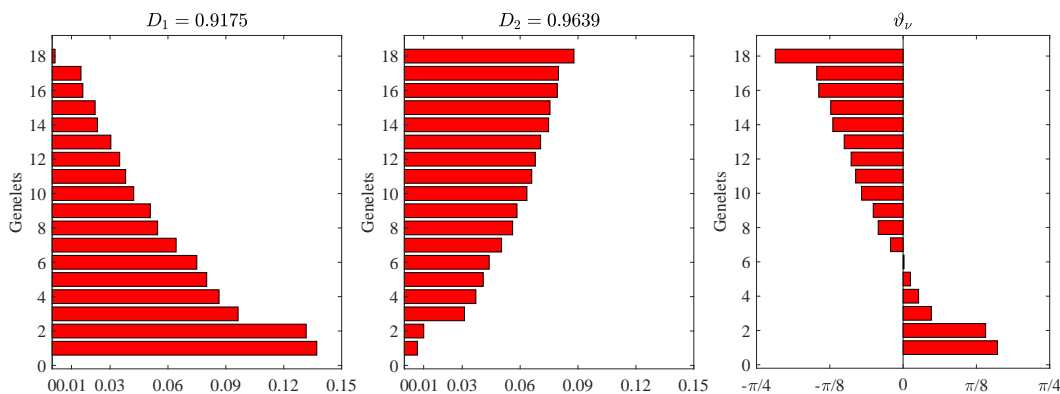
In this data set, the first 2000 genelets are highly significant in PA gene expression relative to the RPMI1640 medium gene expression. The 4500th to 5000th genelets are almost equally significant in both, with a slightly higher significance in the PA gene expression. The 8500th to 9000th genelets are highly significant in the RPMI1640 medium gene expression data. The randomized projection in algorithm 2 mostly benefits from genelets that are significant in one gene expression, where either α_i or β_i is compressible. In many comparative analysis data set, many genelets have biased significantly towards one side. Hence, we conclude algorithm 2 is an efficient algorithm for calculating GSVs of comparative analysis data sets.

5. Conclusion. The target of this paper is to efficiently address the GSV problems in comparative analysis. A randomized GSV algorithm is proposed, where the key is to approximate bases of both G_1 and G_2 matrices by a randomized basis extraction algorithm. By the overall procedure algorithm, generalized fractions of eigenexpression and generalized normalized Shannon entropy for comparative analysis of a class of genome-scale expression data sets can be efficiently computed. The approximation accuracy of the randomized basis extraction algorithm is analyzed. Combined with sensitivity analysis of GSVs, we prove the error analysis of various comparative analysis quantities. Finally, for both synthetic data sets and practical genome-scale expression data sets, we demonstrate that our algorithm outperforms other existing GSV algorithms in runtime. And the accuracy of our algorithm is sufficient for the comparative analysis tasks.

TABLE 3

Absolute errors of algorithm 2 on the yeast and human cell-cycle expression data set with SVD interpolation and spline.

	Absolute error				
	ϑ_ν	D_1	D_2	$P_{1,\nu}$	$P_{2,\nu}$
SVD interpolation	4.13E-14	1.44E-15	1.33E-15	3.55E-15	3.06E-15
Spline	1.99E-14	3.33E-16	6.66E-16	2.47E-15	1.53E-15

FIG. 3. $P_{i,\nu}$, D_i and ϑ_ν computed by algorithm 2 for yeast and human cell-cycle expression data set with SVD interpolation.

REFERENCES

- [1] O. ALTER, P. O. BROWN, AND D. BOTSTEIN, *Singular value decomposition for genome-wide expression data processing and modelling*, Proc. Nat. Acad. Sci., 97 (2000), pp. 10101–10106.
- [2] O. ALTER, P. O. BROWN, AND D. BOTSTEIN, *Generalized singular decomposition for comparative analysis of genome-scale expression data sets of two different organisms*, Proc. Nat. Acad. Sci., 100 (2003), pp. 3351–3356.
- [3] Z. BAI AND J. W. DEMMEL, *Computing the generalized singular value decomposition*, SIAM J. Sci. Comput., 14 (1993), pp. 1464–1486.
- [4] Z. DRMAČ, *A tangent algorithm for computing the generalized singular value decomposition*, SIAM J. Numer. Anal., 35 (1998), pp. 1804–1832.
- [5] L. M. EWERBRING AND F. T. LUK, *Canonical correlations and generalized svd: applications and new algorithms*, Comput. Appl. Math., 27 (1989), pp. 37–52.
- [6] S. FRIEDLAND, *A new approach to generalized singular value decomposition*, SIAM J. Matrix Anal. Appl., 27 (2005), pp. 434–444.
- [7] G. GOLUB AND C. V. LOAN, *Matrix Computations*, Johns Hopkins University Press, Baltimore, 4th ed., 2013.
- [8] N. HALKO, P. G. MARTINSSON, AND J. A. TROPP, *Finding structure with randomness: probabilities algorithms for constructing approximate matrix decompositions*, SIAM Rev., 53 (2011), pp. 217–288.
- [9] R. A. HORN AND C. R. JOHNSON, *Singular value inequalities*, Cambridge University Press, 1991, pp. 134–238.
- [10] C. F. V. LOAN, *Generalizing the singular value decomposition*, SIAM J. Numer. Anal., 13 (1976), pp. 76–83.
- [11] C. F. V. LOAN, *Computing the cs and the generalized singular value decompositions*, Numer. Math., 46 (1985), pp. 479–491.
- [12] P. MARTINSSON AND J. TROPP, *Randomized numerical linear algebra: Foundations and algorithms*, arXiv:2002.01387, (2020).
- [13] C. C. PAIGE, *A note on a result of sun ji-guang: Sensitivity of the cs and gsv decompositions*, SIAM Journal on Numerical Analysis, 21 (1984), pp. 186–191.
- [14] C. C. PAIGE AND M. A. SAUNDERS, *Towards a generalized singular value decomposition*, SIAM J. Numer. Anal., 18 (1981), pp. 398–405.
- [15] G. W. STEWART, *Computing the cs-decomposition of a partitioned orthonormal matrix*, Numer. Math., 40 (1982), pp. 297–306.
- [16] W. XU, M. NG, AND Z. BAI, *Geometric inexact newton method for generalized singular values of grassmann matrix pair*, SIAM J. Matrix Anal. Appl., 43 (2022), pp. 535–560.
- [17] H. ZHA, *A numerical algorithm for computing restricted singular value decomposition of matrix triplets*, Linear Algebra Appl., 168 (1992), pp. 1–25.

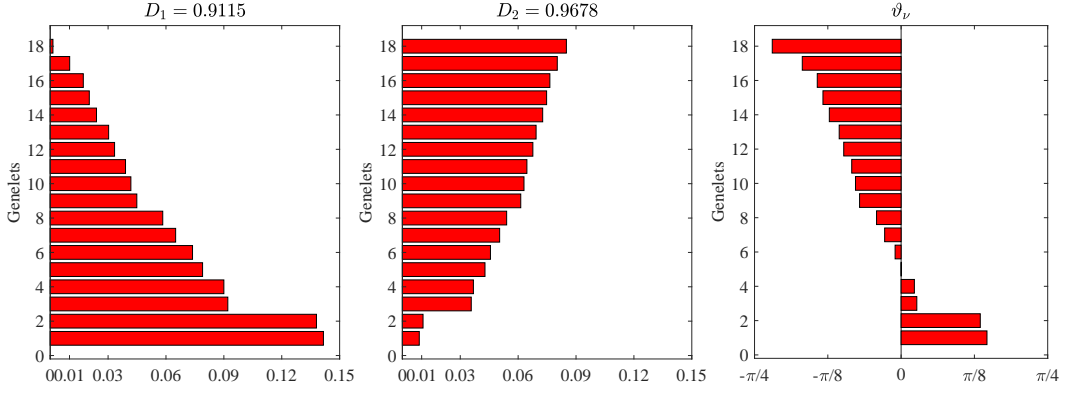


FIG. 4. $P_{i,\nu}$, D_i and ϑ_ν computed by algorithm 2 for yeast and human cell-cycle expression data set with spline.

TABLE 4
Runtime (second) of algorithms on the mice macrophage gene expression data set.

Algorithm	Runtime
algorithm 2	400.06
economy-sized gsvd	40211.43
gsvd	92874.80
Algorithm in [6]	38783.35
RN method [16]	38932.93

TABLE 5
Absolute errors of algorithm 2 on the mice macrophage gene expression data set.

Absolute error				
ϑ_ν	D_1	D_2	$P_{1,\nu}$	$P_{2,\nu}$
4.90E-12	7.21E-12	3.09E-12	6.90E-12	7.03E-12

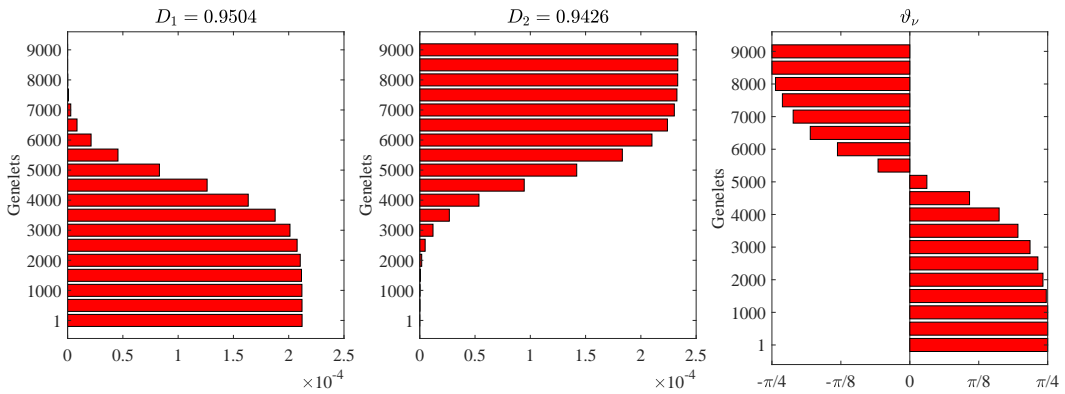


FIG. 5. $P_{i,\nu}$, D_i and ϑ_ν computed by algorithm 2 for mice macrophage gene expression data set.